Semiconductor Physics, Quantum Electronics & Optoelectronics. 2003. V. 6, N 4. P. 471-478.

PACS: 73.63.Bd, 78.55.Ap, 78.67.Bf

Effect of microwave electromagnetic radiation on the structure, photoluminescence and electronic properties of nanocrystalline silicon films on silicon substrate

E.B. Kaganovich, I.M. Kizyak, S.I. Kirillova, R.V. Konakova, O.S. Lytvyn, P.M. Lytvyn,
E.G. Manoilov, V.E. Primachenko, I.V. Prokopenko
V. Lashkaryov Institute of Semiconductor Physics, NAS Ukraine, 41, prospect Nauky, Kyiv, 03028, Ukraine
Phone: +380 (44) 2656182; Fax: +380 (44) 2658342; E-mail: silitech@ukr.net

Abstract. We studied the effect of microwave electromagnetic radiation on silicon low-dimensional structures. The nanocrystalline silicon (*nc*-Si) films on *p*-Si substrate were formed with pulsed laser ablation. The surface morphology of films was studied with atomic force microscopy. We made X-ray phase analysis of films and measured strains in the structures obtained using X-ray diffractometry. We also investigated the time-resolved photoluminescence (PL) spectra and temperature dependence of photovoltage for the *nc*-Si/*p*-Si and *nc*-Si<Au>/*p*-Si structures, both before and after exposure to magnetron microwave radiation of moderate (1.5 W/cm^2) irradiance. It was shown that after microwave irradiation photovoltage in the *nc*-Si films, as well as electron trap concentration in both the films and *p*-Si substrates, decrease. After irradiation of the *nc*-Si/*p*-Si structures the density of interfacial electron states (IES) decreases, while both PL intensity and relaxation time increase. At the same time irradiation of the *nc*-Si<Au>/*p*-Si structures that had high values of PL intensities and relaxation times before irradiation results in decrease of these values, as well as somewhat increases the density of IES. Higher (7.5 W/cm^2) irradiance of microwave field impairs the PL properties (to the point of complete disappearance of PL). In addition it induces changes in film structure resulting, in the course of time, in decrease of strains in the structures studied. We discuss some mechanisms for microwave field effect on the properties of these structures.

Keywords: nanocrystalline silicon, microwave irradiation, photoluminescence, photovoltage, residual strains.

Paper received 05.09.03; accepted for publication 11.12.03.

1. Introduction

Silicon nanocrystals (Si NC) dispersed in a dielectric medium (mostly in silicon oxide SiO$_x$ with $x \leq 2$) form nanocomposites. The latter demonstrate efficient photoluminescence (PL) in the visible spectral range at room temperature. Among such composites are porous silicon (por-Si) formed with chemical etching of single-crystalline silicon (*p*-Si), as well as nanocrystalline silicon (nc-Si) films obtained using sputtering, chemical deposition, implantation, laser ablation and other techniques. These materials offer promise as a basis for development of silicon light-emitting facilities integrable with elements of microelectronics. Investigations of the features of the effect of electromagnetic radiation on the structural, PL and electronic properties of *nc*-Si were performed to develop technological processes for purposeful changes of these properties, as well as for determination of such irradiation conditions at which the above properties still remain stable.

There exist some information on the physical processes in por-Si induced by a high-power laser beam (see, e.g., [1]) and degradation of por-Si PL under ^{60}Co γ-irradiation [2]. However, the effect of microwave (radiofrequency region) electromagnetic radiation on nc-Si and its PL (in the visible spectral region) still remains practically unexplored. At the same time microwave treatments are known to be promising for changing the structural, physico-chemical and electrophysical properties of a number of semiconductor materials and device structures

[3]. The objective of our investigations was to determine how microwave radiation affects the structure, PL spectrum and electronic properties of nc-Si films obtained with pulsed laser deposition onto *p*-Si substrates.

2. Experimental procedure

We obtained PL nc-Si films using the pulsed laser deposition technique [4]. A *Q*-switched YAG:Nd^{3+}-laser had the following operating characteristics: wavelength $\lambda = 1.06\ \mu m$, pulse irradiance of ~20 J/cm^2, pulse duration of 10 ns and repetition rate of 25 Hz. A laser beam scanned a target (made of *c*-Si, grade КДБ-10) without or with a deposited gold film ~80 nm thick (Fig.1). The target and substrate (located in the target plane) were in a vacuum chamber filled with Ar (pressure of ~13 Pa). The interaction between argon atoms and erosion cone particles led to *nc*-Si film deposition from the reverse particle flow onto the *p*-Si substrate. At that size separation of Si NC occurs. At substrate sections located closer to the erosion cone axis the thicker films with bigger Si NC are growing. The film length was 12 mm, and the film thickness varied from 500 down to 50 nm. The film deposition rate varied at different substrate sections from 20 down to 2 nm/min. The film porosity ranged up to 20–30%. For these films the PL spectrum ranged from 1.4 up to 3.2 eV at room temperature.

It was found in earlier works [5,6] that visible PL of these films is determined by the quantum confinement and dielectric effects; the predominant radiation mechanism is annihilation of electron-hole excitations. In [7] it was shown that doping of these films with electropositive metal (gold) leads to increase of PL intensity and shift of PL spectrum to the red region, as well as to increase of the PL relaxation time and stability. These effects were attributed to passivation by gold silicon dangling bonds at the Si NC surface, as well as gold action as a catalyst of NC oxidation [8]. The efficiency of gold action was due to higher values of the first ionization energy and electron affinity of gold atom, as compared to the corresponding values of other metals.

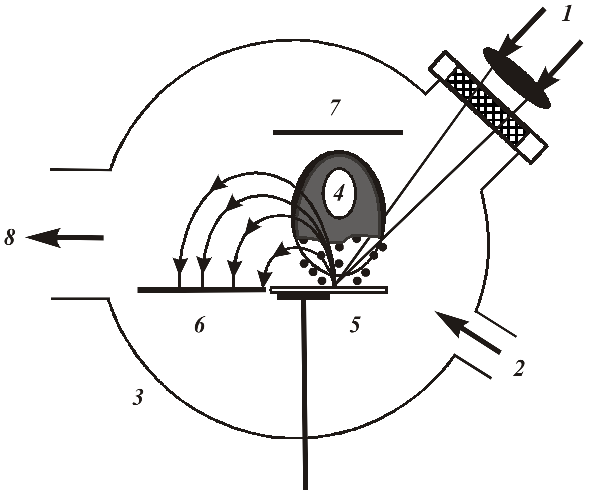

Fig. 1. Schematic of the vacuum chamber used in the PLA technique for nc-Si films: 1 – YAG:Nd^{3+}-laser beam; 2 – gas leak-in; 3 – vacuum chamber; 4 – erosion cone; 5 – target; 6, 7 – substrates; 8 – vacuum pump.

Both undoped and Au-doped samples were exposed to microwave radiation of the cm wavelength range (magnetron, frequency of 2.45 GHz). The output irradiance was 1.5 and 7.5 W/cm^2; time of exposure t_e was varied from 5 up to 15 s.

The film surface morphology was studied with the atomic force microscopy (AFM) using a microscope NanoScope IIIa (Digital Instruments) operating in the tapping mode. Both before and after each measurement the probes were tested using the test structures produced by NT-MDT (Russia). We applied only those probes which had high symmetry and tip radius below 7 nm.

The strains of the *p*-Si substrate near the *nc*-Si/*p*-Si heteroboundary were determined from the results of X-ray diffraction (XRD) measurements of the radius of curvature R of the substrate near-surface crystallographic planes. The strain value was estimated from the relation $\varepsilon \sim t/2R$, t is the substrate thickness. The structure surface profiles were also recorded with a profilometer DEKTAK 3030. The results obtained correlated with those of XRD measurements concerning the structure bending sign.

An attempt to determine phase composition of the films with X-ray technique (using Cu$_{K\alpha}$-radiation and setup with a focusing monochromator) has shown that most of the film volume is an X-ray-amorphous phase. Weak diffraction peaks of polycrystalline silicon, without preferred orientation of Si NC, could be observed against a background of halo due to the above phase. The fraction of silicon oxide was small.

For the *nc*-Si/*p*-Si systems we took (both before and after microwave irradiation) time-resolved PL spectra [5-7] and temperature dependencies of the photovoltage appearing at *nc*-Si/*p*-Si system illumination with light pulses of high intensity [8,9]. PL was excited with nitrogen laser radiation (λ = 337 nm, τ = 8 ns). Stroboscopic registration of a signal was made in the photon-counting mode. The minimal duration of the gate during which photons were collected was 250 ns. The relaxation times below that value were estimated from the oscillograph patterns. Usually the successive gates were registered with a retardation of the measuring gate relative to the laser pulse by an integer number of gate duration. When measuring the maximal (several tens of µs) relaxation times, both gate duration and retardation were arbitrarily increased.

To measure photovoltage, we have installed a measuring capacitor in the vacuum cryostat. This capacitor involved the *p*-Si/*nc*-Si system and mica (pressed to the film) with a semitransparent conducting SnO$_2$<Sb> layer. We measured (*i*) the photovoltage V_{ph} that appeared in the substrate under illumination of the capacitor with pulses of red light, and (*ii*) the total photovoltage in the film and substrate that appeared under illumination with pulses of white light. In the first case (red light), the photovoltage V_{ph} (taken with opposite sign) is equal to the surface potential φ_s of the *p*-Si substrate. The photovoltage was registered using an oscillograph with memory. A flash tube ИСШ-100 (pulse duration of 10 ms, pulse intensity of 10^{21} photons/cm^2·s) served as light source.

3. Results and discussion

The results of our AFM studies of surface morphology of *nc*-Si films are presented in Figs 2 and 3. The films were a nanograin aggregates whose grains consisted of Si NC enveloped with silicon oxide (Fig. 2). The grain size and distribution character were determined by the distance from the erosion cone and the fact if the film has been Au-doped during it deposition. It was also found that if the films were formed from the reverse flow of particles, then their surface was more uniform and grains were smaller as compared to the corresponding characteristics for the case when the films were deposited from the direct flow. The grains in film areas located farther from the erosion cone are smaller, i.e., AFM studies confirmed variation of Si NC sizes along the film (see Fig. 2*a* and *b*, *c* and *d*).

The film surfaces are presented in Fig. 2 as height maps. The height values are reproduced with color gradation in accordance with the scale to the right of the Fig. 2. Shown in Fig. 3*a*, *b* are the quantitative characteristics of these surfaces as relative distributions of the relief heights and grain diameters. One can conclude from Fig. 3*a* that the relief heights for thin film areas (obtained at a distance of about 12 mm from the erosion cone axis) have lower dispersion (± 2 nm), while for thick film areas (obtained closer to the erosion cone axis) the height dispersion is higher (± 6 nm). At that Au-doping does not lead to changes in the relief height distribution.

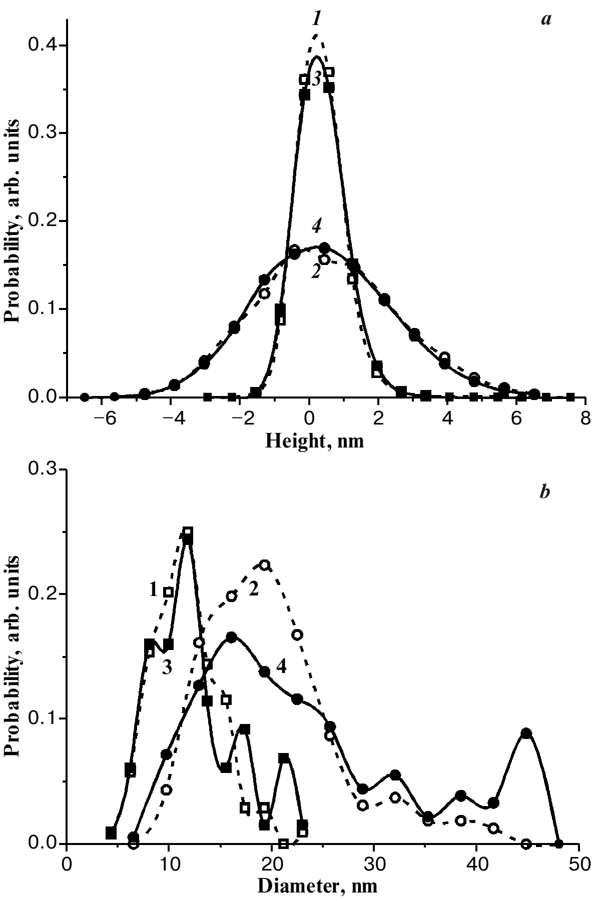

Fig. 3. Relative distribution of relief heights (*a*) and NC diameters (*b*) in nc-Si films (from direct AFM measurements): 1 and 2 – undoped; 3 and 4 – Au-doped thin (1, 3) and thick (2, 4).

One can see from Fig. 3*b* that, as distance from the erosion cone axis grows, the film grain diameters considerably decrease (as well as their dispersion). The undoped films are characterized by more uniform size distribution of grains. Contrary to this, the Au-doped films demonstrate nonuniform size distribution, namely, there are several well-defined characteristic grain sizes in the right section of the plot. This means that gold favors coagulation of some Si NC into larger grains.

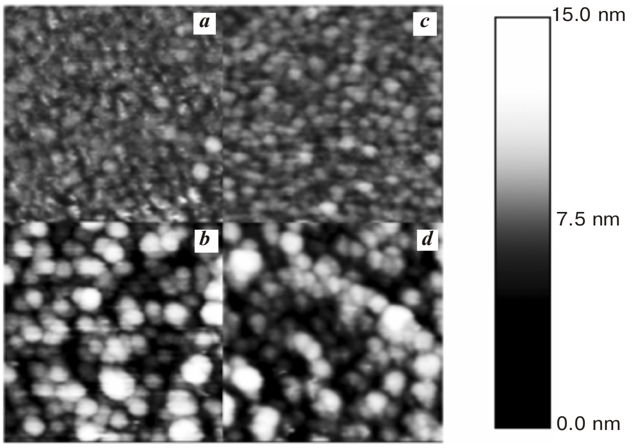

Fig. 2. Surface morphology of *nc*-Si films: *a*, *b* – undoped; *c*, *d* – Au-doped; *a*, *c* – thin with smaller Si NC; *b*, *d* – thick with larger Si NC.

It should be noted that, when AFM-analyzing grains several nm in diameter, the sizes obtained are overestimated due to the effect of "superposition" of the tip form on the relief details (the so-called erosion effect). Knowing tip form from the results of testing, we have made the surface reconstruction procedure (subtraction of the erosion effect). The grain sizes for the reconstructed surface are presented in Table 1.

We believe that the reason for additional coagulation of NC at doping with gold is different substrate conditions at target sputtering with a laser beam. When a substrate (which, after HF treatment, had mainly hydride coating before being placed into the vacuum chamber) is doped with gold, then gold ions and atoms are deposited first of all. They form a surface phase with silicon [8]. This is supported by further data on decrease of the den-

Table 1. Grain diameters determined by direct AFM measurements and after surface reconstruction.

Grain diameter (direct AFM measurements), nm	Grain diameter (reconstructed surface), nm	Degree of diameter overestimation, %
3.20	1.18	63.09
5.42	2.51	53.67
10.00	6.70	41.00
12.80	8.85	30.88
17.83	14.83	16.80
20.62	18.05	12.45
25.06	23.43	6.52

sity of interfacial electron states (IES) at the *nc*-Si<Au>/*p*-Si interface. Thus deposition of silicon particles from the erosion cone onto the substrate with gold and without it proceeds under different conditions. Previously deposited gold favors more intense coagulation of some of Si NC into larger grains.

Both doped and undoped *nc*-Si films deposited onto the *p*-Si substrate are in a nonequilibrium state. Processes of structural ordering are to occur in them under various external actions, in particular, microwave irradiation. AFM studies of the films exposed to microwave radiation (even of the maximal – 7.5 W/cm^2 – irradiance) did not revealed noticeable changes in their surface morphology. The results of high information ability have been obtained, however, when measuring radius of curvature for the *p*-Si, *p*-Si/nc-Si and *p*-Si/nc-Si<Au> samples with XRD technique (Fig. 4). For the samples consisting of the *p*-Si substrate only, the radius of curvature R was about 30 m; the samples were convex toward the side at which the nc-Si films were later deposited (curvature sign “plus”). The calculation gave for the strain ε the value of about $5 \cdot 10^{-6}$. Stressed state of the initial substrate was due to different treatments of its sides. That used for nc-Si films deposition was at first chemo-dynamically treated, then treated in HF and washed in water. As a result, it had a hydride coating that, being exposed to air, gradually gave place to a thin oxide film. Another side of the substrate experienced only mechanical lapping before the HF treatment. One can see from Fig. 4 that the radius of curvature of the *p*-Si substrate practically did not change after microwave irradiation followed by keeping out of doors.

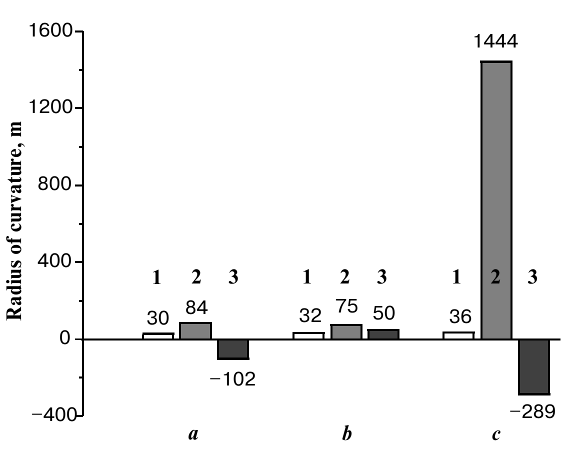

Fig. 4. Variation dynamics for radii of curvature of structures: 1 – substrate; 2 – substrate with undoped film; 3 – substrate with Au-doped film. *a* – initial; *b* – after microwave irradiation for 5 s; *c* – after further keeping out of doors for 120 h.

After deposition of an undoped nc-Si film onto the *p*-Si substrate, the strain in the system studied dropped (R = 84 m). Microwave irradiation somewhat increased strain (R = 75 m), but then, after keeping the sample out of doors for 120 h, strains strongly relaxed (the radius of curvature grew up to 1444 m). Very interesting results were obtained after deposition of an nc-Si<Au> film onto the substrate. In this case the radius of curvature changed its sign, i.e., the nc-Si<Au>/*p*-Si system became concave toward the film, and its strain considerably decreased (R = –102 m). This fact can be related to both the above mechanism for a gold-silicon phase formation at the film/substrate interface and thermal strains caused by distinction between the film and substrate thermal expansion coefficients.

Changes of sign and value of the radius of curvature immediately after microwave irradiation (R = 50 m) seems to result from both disordering of the above surface phase and structure defects redistribution under microwave field action. However, during keeping samples out of doors that phase restores and metastable defect clusters dissociate. As a result, the radius of curvature becomes negative again, and its magnitude substantially increases (R = –289 m). Thus in both cases (undoped and Au-doped films on the *p*-Si substrate) microwave irradiation induces processes of structure relaxation proceeding after it. As a result, the residual strains in the *nc*-Si/*p*-Si and nc-Si<Au>/*p*-Si systems drop abruptly.

Fig. 5 shows the time-resolved PL spectra for undoped (*a*) and Au-doped (*b*, *c*, *d*) films before (curve 1*a* and Fig. 5*b*) and after (curves 2–4 in Fig. 5*a* and curves in Figs. 5*c* and 5d) microwave irradiation. The spectra range from 1.4 up to 3.2 eV. In our previous works [5–7] we gave interpretation of the PL spectra of these films before microwave irradiation depending on the formation condition, as well as explained spectra transformation during PL relaxation. For the undoped *nc*-Si/*p*-Si structure the character of PL spectral dependence practically did not change after microwave irradiation. The PL intensity, however, at moderate (1.5 W/cm^2) irradiance increased by a factor of 2–3 with time of sample exposure t_e in microwave field (Fig. 5a, curves 2 and 3 t_e = 5 and 15 s). At bigger irradiance (7.5 W/cm^2, t_e = 15 s) the PL intensity decreased (curve 4). The PL relaxation time t (which is determined mainly by the time of nonradiative recombination of nonequilibrium electron-hole pairs) varied with PL intensity. After exposure to moderate microwave irradiance the PL relaxation time grew from 50 up to 100–

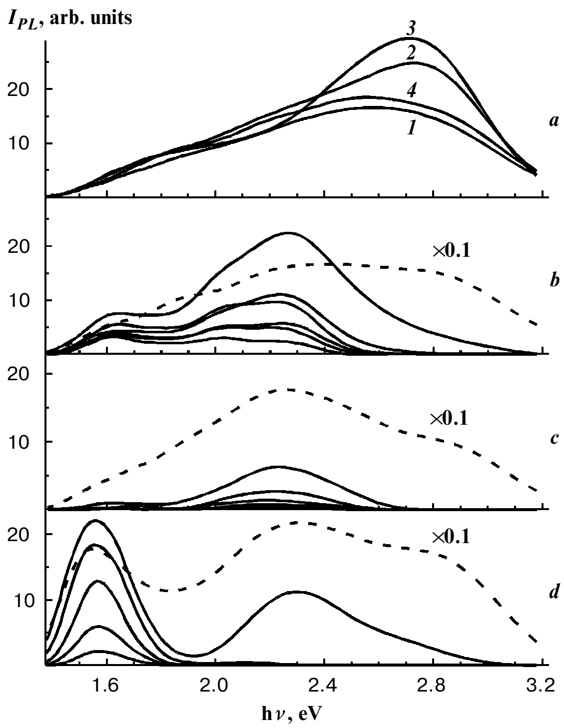

Fig. 5. Time-resolved PL spectra of undoped (*a*) and Au-doped (*b*, *c*, *d*) *nc*-Si/*p*-Si structures before (curves 1*a*, *b*) and after (curves 2–4*a*, c, d) microwave irradiation with irradiance of 1.5 W/cm^2 (curve 4a – 7.5 W/cm^2). Time of exposure 15 s (curve 2*a* – 5 s). Curves *a* and broken curves *b*, *c*, *d* were obtained in the $\tau <$ < 250 ns gate. Full curves *b*, *c*, *d* are given for further gates; the lowest curves correspond to the PL relaxation times of 1.8, 1.2 and 12 μs. The structure *d* was aged out of doors.

200 ns, and after strong (irradiance of 7.5 W/cm^2) microwave action it dropped to several tens of ns.

All the spectral curves in Fig. 5*a* were taken during the first gate of PL relaxation ($t < 250$ ns). For Au-doped structures (where the PL relaxation time increased almost by three orders of magnitude) the PL spectra before (Fig. 5*b*) and after (Fig. 5*c*, *d*) microwave irradiation are presented for two different gates. The spectra obtained during the first gate (their intensities are decreased by a factor of ten) are shown with broken curves. Full curves corresponding to higher intensities $I_{\rm PL}$ represent the spectra obtained during the second gate (250 ns < τ < 500 ns), while the curves corresponding to lower $I_{\rm PL}$ values show the spectra obtained during further gates. (In Figs. 5*b*, *c*, *d* the curves corresponding to the lowest $I_{\rm PL}$ values were obtained for the PL relaxation times of 1.8, 1.2 and 12 μs, respectively).

Contrary to undoped structure, irradiation of as-prepared *nc*-Si<Au>/*p*-Si structure with microwave field (1.5 W/cm^2, t_e = 15 s) results in impairment of PL parameters (Fig. 5*c*): (*i*) the integral (i.e., sum over all the PL components with different relaxation times) PL intensity becomes several times below; (*ii*) the PL relaxation time goes down to 1 μs; (*iii*) the spectrum is modified, first of all, due to intensity drop for the low-energy band. After irradiation with microwave field (irradiance of 7.5 W/cm^2, t_e = 15 s) PL disappears completely.

Another situation was realized after microwave irradiation (irradiance of 1.5 W/cm^2, t_e = 15 s) of an Au-doped structure that previously was kept out of doors for 8 months, i.e., was aged. The spectra of such structure after microwave irradiation are presented in Fig. 5*d*. In this case the structure is more tolerant to action of microwave field: the PL relaxation time remains sufficiently high (~20 μs); the PL intensity dropped but slightly, especially in the low-energy region (~1.6 eV) where an intense PL band was observed both before and after irradiation.

When measuring the temperature dependencies of the capacitor photovoltage V_{ph}, we illuminated the nc-Si/*p*-Si structures alternately by red and white light pulses. Figures 6a, b show the $V_{ph}(T)$ curves for undoped and Au-doped structures, respectively (the photovoltage at the semitransparent SnO$_2$<Sb> electrode was negative). The curves 1, 1′, 2 and 2′ were obtained before microwave

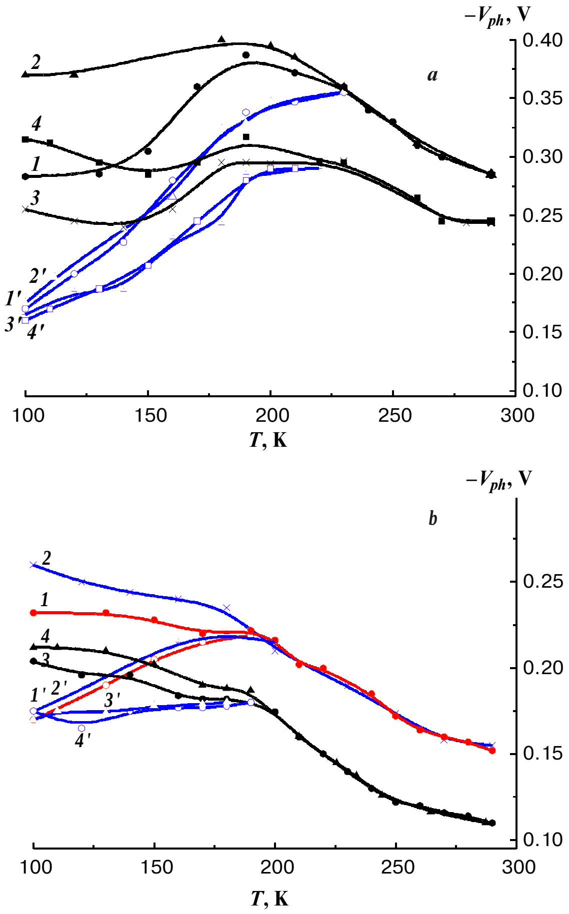

Fig. 6. Photovoltage for undoped (*a*) and Au-doped (*b*) structures as function of temperature: 1, 1′, 2, 2′ – before, 3, 3′, 4, 4′ – after microwave irradiation at the first (1, 2, 3, 4) and second (1′, 2′, 3′, 4′) pulses of red (1, 1′, 3, 3′) and white (2, 2′, 4, 4′) light.

irradiation of the structures; the curves 3, 3′, 4 and 4′ were obtained after microwave irradiation, at the first (1, 2, 3 and 4) and second (1′, 2′, 3′ and 4′) pulses of red (1, 1′, 3 and 3′) and white (2, 2′, 4 and 4′) light.

The curves 1, 1′, 3 and 3′ show variation of the potential $\varphi_s = -V_{ph}$ at the *p*-Si substrate boundary with temperature. The V_{ph} values measured at the second pulse (or any next pulse from their group) had lower magnitude than those measured at the first pulse. This effect was observed starting from certain temperatures (which were somewhat different for different structures) with their further decreasing. This means that at low temperatures the optical memory effects exist [10]. They are due to trapping of electrons by traps located at the *p*-Si substrate/nc-Si film interface (at illumination with red light) or by both the above traps and those in the film (at illumination with white light). In presence of the optical memory effects the measurements were made with warming the samples up (see [9, 11, 12].

One can see from Fig.6 that the $V_{ph}(T)$ curves change as a result of microwave irradiation (1.5 W/cm^2, 15 s). The corresponding $|V_{ph}|$ values at the same temperatures decrease, and the very character of the curves changes, especially for the undoped structure. For all the curves at $T >$ 200–240 K the V_{ph} values obtained at illumination with red and white light are the same. This is evidence that no considerable photovoltage appears at such temperatures in the nc-Si films illuminated with pulses of white light whose high-energy part is absorbed in them. Increase of $|V_{ph}|$ at lowering temperature in that region is due to charging of IES of the *p*-Si substrate with holes when the Fermi level in the silicon bulk goes to the valence band. The calculations (similar to those made in [10]) showed that before microwave irradiation the Fermi level in *p*-Si was practically pinned near the Si midgap E_i due to high (over 10^{12} cm$^{-2}\cdot$eV^{-1}) density of IES at the *p*-Si/undoped nc-Si film interface. After microwave irradiation the density of IES decreases considerably and is about $3\cdot10^{11}$ cm$^{-2}\cdot$eV^{-1} near E_i.

One can see from the $V_{ph}(T)$ curves (Fig. 6*a*) obtained at the first red light pulses (curves 1 and 3) that, starting from certain temperature, the $|V_{ph}|$ values begin to decrease when temperature goes down. Such decrease of $|V_{ph}| = \varphi_s$ is related to transformation of the IES system due to reversible structure changes at the *nc*-Si/*p*-Si interface [11]. For structures exposed to microwave irradiation decrease of j_s gives place to its growth at $T <$ 120–140 K (curve 3). This results from the competition between the processes of transformation of the IES system and charging IES with holes as temperature varies.

No transformation of the IES system was observed for the aged Au-doped *nc*-Si/*p*-Si structure over the whole temperature range studied (300–100 K), both before and after microwave irradiation (Fig. 6*b*, curves 1 and 3). This makes it possible to study, as temperature varies, a wider portion of the silicon gap and calculate the density of IES in that range [10]. Fig. 7 shows the density of IES below E_i in the energy range 0.14–0.31 eV before (curve 1) and after (curve 2) microwave irradiation of the *nc*-Si<Au>/*p*-Si structure. One can see that before microwave irradiation two discrete levels – at E_i – 0.18 eV and E_i – 0.23 eV – show themselves. The corresponding densities of state are $3.2\cdot10^{11}$ and $4\cdot10^{10}$ cm$^{-2}\cdot$eV^{-1}.

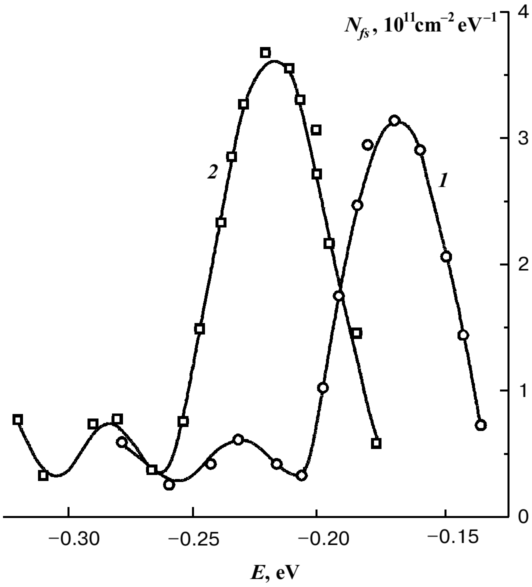

Fig. 7. Density of IES at Au-doped structure below the silicon midgap E_i: 1 – before, 2 – after microwave irradiation.

It should be noted that the density of IES after doping wit Au is low. This is related to formation of a gold-silicon phase at the *p*-Si substrate surface [8]. After microwave irradiation these levels shift from E_i. Their energy positions become E_i – 0.23 eV and E_i – 0.27 eV, while the corresponding densities increase up to $3.8\cdot10^{11}$ and $5.8\cdot10^{10}$ cm$^{-2}\cdot$eV^{-1}, respectively. Thus moderate microwave irradiation decreases the density of IES at the *p*-Si substrate for the undoped structure and somewhat increase it for the Au-doped structure.

One can see from Fig. 6 that the $|V_{ph}|$ values measured at structure illumination with the first pulses of white and red light begin to differ only at certain temperatures with

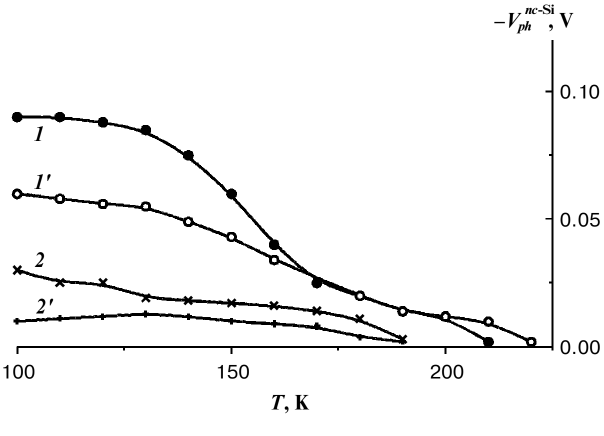

Fig. 8. Photovoltage for nc-Si films of undoped (1, 1′) and Au-doped (2, 2′) structures as function of temperature: 1, 2 – before, 1′, 2′ – after microwave irradiation.

their going down. This indicates that at these low temperatures a photovoltage $V_{ph}^{nc\text{-Si}}$ appears in the *nc*-Si films. It is a difference between the V_{ph} values obtained under illumination with white and red light at the same temperature. The photovoltage $V_{ph}^{nc\text{-Si}}$ is negative; its sign is the same as that of the photovoltage in the substrate.

Shown in Fig. 8 are the temperature dependencies of photovoltage $V_{ph}^{nc\text{-Si}}$ for undoped (curves 1 and 1′) and Au-doped (curves 2 and 2′) structures measured before (curves 1 and 2) and after (curves 1′ and 2′) microwave irradiation. The very appearance of photovoltage in the films as temperature decreases, as well as its variation with temperature, evidence that appearance of photovoltage is due reversible stresses in the films that appear as temperature goes down. These stresses induce a built-in positive charge which increases when approaching the outer surface of the film. The electron-hole pairs produced in the film by white light are separated by the electric field of the above charge, and this leads to appearance of photovoltage in the film. The lower is photovoltage in the Au-doped films, the smaller are stresses in the films. After microwave irradiation of the structures, the magnitudes of photovoltage decrease for all films (Fig. 8). This fact also indicates at reduction of stresses in the films after microwave irradiation as temperature goes down.

Fig. 9*a* presents temperature dependencies of the concentrations $N^{p\text{-Si}}$ of electrons trapped by the traps at the *p*-Si substrate boundary. The $N^{p\text{-Si}}(T)$ curves were calculated (as in [9]) from the difference between the curves 1 and 1′, 3 and 3′ (Fig. 6) taken at the red light pulses. The dependencies $N^{p\text{-Si}}(T)$ were obtained for undoped (curves 1 and 1′) and Au-doped (curves 2 and 2′) structures before (curves 1 and 2) and after (curves 1′ and 2′) microwave irradiation. The traps are completely filled with electrons during the first light pulse. Therefore the $N^{p\text{-Si}}(T)$ curves also describe temperature dependence of the electron trap concentrations at the substrate. Growth of these concentrations as temperature goes down results from the fact that shallow-lying traps (which are closer to the conduction band of silicon) begin to take part in electron trapping. One can see from Fig. 9*a* that for all the structures studied the concentrations of traps at the substrate dropped after microwave irradiation.

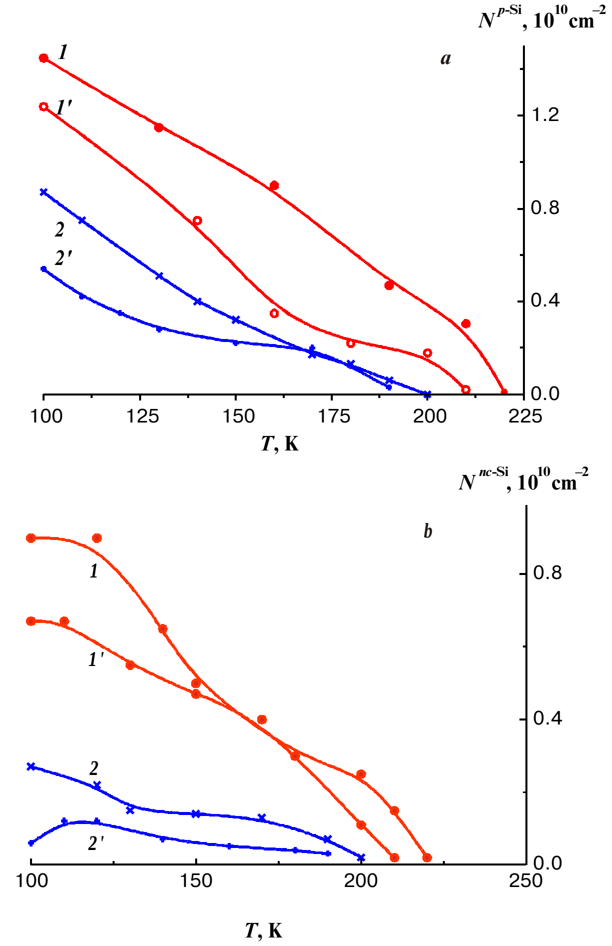

Fig. 9. Temperature dependencies of the concentrations of trapped nonequilibrium electrons for *p*-Si substrate (*a*) and *nc*-Si film (*b*) in undoped (1, 1′) and Au-doped (2, 2′) structures: 1, 2 – before, 1′, 2′ – after microwave irradiation.

Shown in Fig. 9*b* are the temperature dependencies of the concentrations $N^{nc\text{-Si}}$ of nonequilibrium electrons captured by the traps in the nc-Si films. These dependencies were calculated using the curves 2 and 2′, 4 and 4′ (Fig. 6) taken at the white light pulses (the concentration of electrons captured by the traps at the *p*-Si substrate was subtracted). It should be noted that in our calculations of $N^{nc\text{-Si}}$ we determined the lower bound to the number of electrons captured by the traps in the film, because drop of potential (produced by the charge of trapped electrons) takes place not only in the substrate but in the film as well. The traps in the film, as those at the substrate, were completely filled with electrons during the first pulse of white light. Therefore the $N^{nc\text{-Si}}(T)$ curves also show the temperature dependencies of the electron trap concentration in the film. One can see from Fig. 9*b* that for all the structures studied the trap concentration in the *nc*-Si film decreases after microwave irradiation over almost the whole temperature range. Thus, for both undoped and Au-doped *nc*-Si/*p*-Si structures, moderate microwave irradiation decreases concentration of traps for nonequilibrium electrons at the *p*-Si substrates, as well as in the *nc*-Si films.

4. Some concluding remarks

Summing up the results obtained, we would like to note that variation of the properties of *nc*-Si/*p*-Si structures exposed to microwave irradiation depends, on the one hand, on the microwave irradiance and time of exposure, and, on the other hand, on the initial (before irradiation) structure properties. High microwave irradiance results in degradation of some structure properties (say, PL reduction for undoped structure and complete suppression of PL for Au-doped structure at microwave irradiation with irradiance of 7.5 W/cm^2). At the same time moderate (1.5 W/cm^2) irradiance can impair, as well as improve, structure parameters. For instance, after moderate action of microwave field the following improvements are observed:

- both PL intensity and PL relaxation time increase for undoped structure;
- density of IES at the substrate decreases for undoped structure;
- for all structures concentration of traps for nonequilibrium electrons decreases, both at the substrate and in the nc-Si film;
- strains in the *nc*-Si film and at the film/substrate interface decrease as temperature goes down (this follows from photovoltage decreasing in the film and variation of the character of $\varphi_s(T)$ curves for undoped structure after microwave irradiation).

At the same time moderate microwave action impairs some parameters of the Au-doped *nc*-Si/*p*-Si structure, namely:

- both PL intensity and relaxation time decrease;
- density of IES at the *p*-Si substrate somewhat increases.

These changes occur for the structure which (due to Au-doping) demonstrated much better parameters than the undoped structure, even before microwave irradiation. It should be noted that PL of aged *nc*-Si<Au>/*p*-Si structure is more tolerant to microwave action, due to more complete oxidation of Si NC when keeping out of doors.

The changes occurring in the *nc*-Si/*p*-Si structures during microwave irradiation may result from several factors. First, microwave field is heating up charge carriers in both the *p*-Si substrate and Si NC. At high energies and concentrations of these charge carriers (which are obtained at high microwave irradiance) they produce local defects, in particular, silicon dangling bonds. This results in decrease, or even complete suppression, of PL. Contrary to this, at moderate microwave irradiance (when local defect production is insignificant) the principal role of heated charge carriers is in transfer of their energy to silicon crystal lattice as a whole. Heating of the lattice leads to structure changes in the nc-Si film, as well as at the film/substrate interface: the nonequilibrium structures (obtained under laser ablation) become more ordered. This can explain reduction of stresses in the films and at their interfaces with the substrate, which can be seen immediately from XRD studies.

Besides, structure annealing that occurs under moderate microwave irradiation also leads to reduction of the electron trap concentration in the film and at the substrate, as well as to reduction of the density of IES. It is likely that these positive actions of moderate microwave irradiations are supplemented with afteroxidation of Si NC that occurs at microwave action out of doors. This results in PL growth for the undoped structure where (contrary to the nc-Si<Au>/*p*-Si structure) both PL intensity and relaxation time were small before microwave irradiation.

In conclusion we would like to stress that consequences of the action of any electromagnetic radiation of low irradiance (dose, intensity) depend on the degree of ordering (equilibrium) of the system under action. If the system is in equilibrium, then even moderate (in irradiance, dose or intensity) radiation can impair its parameters. On the contrary, moderate irradiation often improves parameters of a non-equilibrium (disordered) system, as was observed in [1–3]. The above statements are also supported by the results of this work.

References

1. Yu.A. Bykovsky, V.A. Karavansky, G.E. Kotkovsky, M.B. Kuznetsov, A.A. Chistyakov, A.A. Lomov, S.A. Gavrilov, Photophysical processes induced in nanoporous silicon by high-power laser radiation // *Zhurn. Eksper. Teor. Fiz.* **117**(1), pp. 136-144 (2000) (in Russian).
2. E.V. Astrova, R.F. Vitman, V.V. Emtsev, A.A. Lebedev, D.S. Poloskin, A.D. Remenyuk, Yu.V. Rud', Effect of γ-irradiation on the properties of porous silicon // *Fiz. Tekhn. Poluprov.* **30**(3), pp. 507-515 (1996) (in Russian).
3. A.E. Belyaev, A.A. Belyaev, E.F. Venger, I.B. Ermolovich, S.M. Komirenko, R.V. Konakova, V.G. Lyapin, I.I. Magda, V.V. Milenin, I.V. Prokopenko, S.V. Svechnikov, E.A. Soloviev, Yu.A. Tkhorik, M.V. Shevelev, Effect of microwave radiation on structural, physico-chemical and electrophysical properties of a number of semiconductor materials and device structures. In: *6th Intern. Crimean Conf. "Microwave & Telecommunication Technology", Conf. Proc.*, Sevastopol, Weber Co., pp. 71-89 (1996) (in Russian).
4. L. Patrone, D. Nelson, V.I. Safarov, M. Sentis, W. Marine, S. Giorgio, Photoluminescence of silicon nanoclusters with reduced size dispersion produced by laser ablation // *J. Appl. Phys.* **87**(8), pp. 3829-3837 (2000).
5. E.B. Kaganovich, E.G. Manoilov, S.V. Svechnikov, The role of oxygen in radiative recombination of nanocrystalline silicon // *Ukr. Fiz. Zhurn.* **46**(11), pp. 1196-1201 (2001) (in Ukrainian).
6. A.V. Sachenko, E.B. Kaganovich, E.G. Manoilov, S.V. Svechnikov, Kinetics of excitonic photoluminescence in low-dimensional silicon structures // *Fiz. Tekhn. Poluprov.* **35**(12), pp. 1445-1451 (2001) (in Russian).
7. E.B. Kaganovich, I.M. Kizyak, E.G. Manoilov, V.E. Primachenko, S.V. Svechnikov, Doping of inside of porous silicon films with gold ions // *Ukr. Fiz. Zhurn.* **47**(7), pp. 680-683 (2002) (in Ukrainian).
8. V.E. Primachenko, O.V. Snitko, *Physics of Semiconductor Surface Doped with Metals,* Naukova Dumka, Kiev (1988) (in Russian).
9. E.F. Venger, E.B. Kaganovich, S.I. Kirillova, E.G. Manoilov, V.E. Primachenko, S.V. Svechnikov, Investigation of porous silicon/silicon structures with the photovoltage temperature curves technique // *Fiz. Tekhn. Poluprov.* **33**(11), pp. 1330-1333 (1999) (in Russian).
10. E.F. Venger, S.I. Kirillova, V.E. Primachenko, V.A. Chernobai, Surface electron state system of thermally oxidized and real silicon surfaces // *Ukr. Fiz. Zhurn.* **42**(11/12), pp. 1333-1339 (1997) (in Ukrainian).
11. S.I. Kirillova, V.E. Primachenko, O.V. Snitko, V.A. Chernobai, Electronic properties of silicon surface at its different physicochemical states // *Poverkhnost'* No 11, pp. 74-79 (1991) (in Russian).
12. S.I. Kirillova, V.E. Primachenko, V.A. Chernobai, Optical memory effect of surface potential under different silicon surface conditions // *Optoelektr. i Poluprov. Tekhn.* No 21, pp.60-63 (1991) (in Russian).